BIOELECTRICITY
Volume 5, Number 4, 2023

DOI: 10.1089/bioe.2022.0036

Endoplasmic Reticulum Calcium Mediates *Drosophila* Wing Development

Laura Faith George, PhD, Mikaela Lynn Follmer, Emily Fontenoy, Hannah Rose Moran, Jeremy Ryan Brown, Yunus H. Ozekin, MS, and Emily Anne Bates, PhD

Abstract

Background: The temporal dynamics of morphogen presentation impacts transcriptional responses and tissue patterning. However, the mechanisms controlling morphogen release are far from clear. We found that inwardly rectifying potassium (Irk) channels regulate endogenous transient increases in intracellular calcium and bone morphogenetic protein (BMP/Dpp) release for *Drosophila* wing development. Inhibition of Irk channels reduces BMP/Dpp signaling, and ultimately disrupts wing morphology. Ion channels impact development of several tissues and organisms in which BMP signaling is essential. In neurons and pancreatic beta cells, Irk channels modulate membrane potential to affect intracellular Ca^{++} to control secretion of neurotransmitters and insulin. Based on Irk activity in neurons, we hypothesized that electrical activity controls endoplasmic reticulum (ER) Ca^{++} release into the cytoplasm to regulate the release of BMP.

Materials and Methods: To test this hypothesis, we reduced expression of four proteins that control ER calcium, Stromal interaction molecule 1 (Stim), Calcium release-activated calcium channel protein 1 (Orai), SarcoEndoplasmic Reticulum Calcium ATPase (SERCA), small conductance calcium-activated potassium channel (SK), and Bestrophin 2 (Best2) using RNAi and documented wing phenotypes. We use live imaging to study calcium and Dpp release within pupal wings and larval wing discs. Additionally, we employed immunohistochemistry to characterize Small Mothers Against Decapentaplegic (SMAD) phosphorylation downstream of the BMP/Dpp pathway following RNAi knockdown.

Results: We found that reduced Stim and SERCA function decreases amplitude and frequency of endogenous calcium transients in the wing disc and reduced BMP/Dpp release.

Conclusion: Our results suggest control of ER calcium homeostasis is required for BMP/Dpp release, and *Drosophila* wing development.

Keywords: calcium, transients, endoplasmic reticulum, SERCA, Stim, Orai, bestrophin, *Drosophila* wing development, wing venation, BMP, bone morphogenic protein

Introduction

CELLS COMMUNICATE WITH each other to orchestrate cell division, differentiation, and migration to reproducibly shape tissues, and ultimately organisms. Decades of research have elucidated a multitude of molecular pathways that cells use to communicate. Cells secrete morphogens that bind to receptors that activate transcription factors to control tissue patterning. A set of highly conserved molecular pathways such as the bone morphogenetic protein (BMP), Notch, Hedgehog (Hh), Wnt, and epidermal growth factor signaling work together to repeatedly instruct patterning in a diverse range of tissues in vertebrates and invertebrates.[1] For example, BMP/Dpp signaling guides dorsal–ventral (D/V) patterning in the *Drosophila* embryo, and later regulates growth and patterning of many adult structures, including the wing at larval and pupal stages.[2–6]

BMP ligands bind a complex of type 1 and type 2 serine threonine kinase receptors.[7] Upon ligand binding, type 1 receptors phosphorylate Small Mothers Against Decapentaplegic that can then enter the nucleus to affect transcription. This pathway and its roles are conserved from flies to

Department of Pediatrics, University of Colorado Anschutz Medical Campus, Aurora, Colorado, USA.

mammals.[8,9] Considering the relatively small number of molecular signaling pathways that guide development of diverse tissue architectures, each signal must be spatially and temporally regulated. This study seeks to understand how cells deliver ligands at the correct time and place to control diverse complex developmental processes.

We found that BMP/Dpp release is regulated by inwardly rectifying potassium (Irk) channels for proper development of the *Drosophila* wing suggesting that cells could precisely control temporal delivery of developmental signals using bioelectricity, mediated by ion channels. Ion channels are required for morphogenesis in a wide variety of organisms ranging from planarians to humans, suggesting a conserved role for bioelectricity in development.[10–16] In planarians, gap junction channels are required for directing the body plan of regenerating planaria, and disruption of gap junction function can result in the growth of double-headed organisms.[17] A screen of ion channels in *Drosophila melanogaster* showed that at least 44 different ion channels are required for proper development of the *Drosophila* wing.[12] Similarly, genetic disruption of ion channels causes morphological abnormalities in zebrafish,[15,18] chickens,[19] mice,[16,20] and humans.[21–32] Together, these studies and others provide strong evidence that ion channels play an important role in development.

In excitable cells, such as neurons and pancreatic beta cells, ion channels modulate membrane potential to control intracellular Ca^{++} to regulate secretion of neurotransmitters and insulin.[33–39] Based on ion activity in other excitable cells, we hypothesized that electrical activity mediates intracellular Ca^{++} dynamics to regulate the release of BMP. Thus, ion channels could provide precise temporal presentation of molecular signals for developmental signaling.

In support of this hypothesis, we found transient increases in intracellular calcium in the wing disc (wing primordia) cells, when BMP/Dpp signaling is active. Inhibition of Irk channels alters Ca^{++} transients, BMP/Dpp release dynamics, activation of BMP/Dpp targets, and ultimately wing morphology.[20,40] Endogenous calcium waves and transients have been found in diverse developing tissues in multiple organisms including developing blue pansy butterflies,[41] developing *Drosophila* wings and air sac primordium (ASP),[42–46] zebrafish,[47] *Xenopus*,[47,48] and chick feather buds.[19] Calcium oscillations are classified into four different groups: single cell transients, short distance intracellular transients, long-distance calcium waves, and rapid low amplitude calcium oscillations called ''fluttering.''[45] Abolishment of calcium transients disrupts normal development, suggesting that they have a critical role.[19,41]

Ion channels are important for the proper trafficking and release or surface presentation of signaling pathway components. Disruption of Irk2/Kir2.1 disrupts intracellular calcium[40] and disrupts the secretion dynamics of BMP/Dpp, reducing BMP/Dpp signaling, and causing wing developmental defects.[12,20,40] These results suggest that intracellular calcium dynamics may be important for BMP/Dpp secretion.[40] In the *Drosophila* ASP, disruption of Syt4 or synaptobrevin (Syb), two calcium binding proteins involved in vesicle trafficking, disrupts BMP/Dpp signaling, suggesting that calcium-mediated vesicular trafficking may be important for BMP/Dpp secretion.[46] Together, these data led us to evaluate the role of intracellular calcium modulation of the BMP signaling pathway.

Transient increases in intracellular calcium concentration could come from extracellular calcium or release from the endoplasmic reticulum (ER). ER calcium stores are tightly regulated. Stim and Orai are calcium release activated channels (CRAC) that respond to decreases in ER calcium levels by mediating re-entry of calcium into the cell.[49,50] Sarco-Endoplasmic Reticulum Calcium ATPase (SERCA) is an ER calcium pump that maintains ER calcium homeostasis.[51] Small conductance calcium-activated potassium channel (SK) that activates in response to increases in intracellular calcium to conduct outward flow of potassium, offsetting the effect of increased intracellular calcium on the transmembrane potential.[52] Finally, Best2 is a calcium-activated chloride channel. A Bestrophin mammalian homolog acts in the ER to counterbalance calcium release and augment intracellular calcium transients, but little is known about the function of Best2 in *Drosophila*.[53,54]

Here, we show that during both the larval and pupal stages, developing *Drosophila* wings have spontaneous calcium transients. At the larval stage these calcium oscillations can be abolished by treatment with the SERCA inhibitor thapsigargin, or by RNAi knockdown of SERCA or Stim, suggesting that these oscillations are mediated by ER calcium stores. Disruption of SERCA or Stim disrupts BMP/Dpp secretion dynamics suggesting a mechanism by which ER calcium may impact developmental signaling. Together our results suggest that ER calcium regulation is important for the BMP signaling pathway to drive proper patterning and development of the *D. melanogaster* wing.

Materials and Methods

Fly Stocks and wing imaging

The Bloomington *Drosophila* Stock Center supplied all fly lines used including MS1096-gal4 (*w[1118] P[GawB-DeltaKE]Bx[MS1096-KE]*; BDSC #8696), nub-gal4 (*w[*]; P[w[nub.PK]=nub-GAL4.K]2*; BDSC 86108), dpp-gal4 (*w[*]; wg[Sp-1]/CyO; P[w[+mW.hs]=GAL4-dpp.blk1]40C .6/TM6B, Tb[1]*; BDSC 1553), SERCA RNAi (*y[1] w[67c23]; P[y[+mDint2] w[BR.E.BR]=SUPor-P]SERCA[KG00570]*; BDSC #25928), Orai RNAi (*y[1] sc[*] v[1] sev[21]; P[y[+t7.7] v[+t1.8]=TRiP.HMC03562]attP40*; BDSC 53333), Stim RNAi (*y[1] v[1]; P[y[+t7.7] v[+t1.8]=TRiP.JF02567] attP2*; BDSC #27263), SK RNAi (*y[1] v[1]; P[y[+t7.7] v[+t1.8]=TRiP.HMJ21196]attP40*; BDSC #53881), Best2 RNAi (*y[1] sc[*] v[1] sev[21]; P[y[+t7.7] v[+t1.8]= TRiP.HMS02490]attP2*; BDSC #42654), and calcium reporter, Green fluorescent protein, calmodulin, and myosin light chain kinase (GCaMP7s) (*w[1118]; P[y[+t7.7] w[+mC]=20XUAS-IVS-jGCaMP7s]su(Hw)attP5*; BDSC #80905).

Flies were raised at 25°C on standard cornmeal food using recipe as described by Hazegh and Reis.[55] Wings for each of the RNAi lines were dissected and mounted on slides and wings were imaged using a histology microscope (eclipse 80I; Nikon). The MS1096-gal4 driver is on the X chromosome, and thus male flies are hemizygous for the MS096-gal4 driver and have a higher dosage of any expressed RNAi than female flies. For consistency, all wing images were taken from female flies.

Immunofluorescence

To collect larvae and pupae for dissection, egg collections were restricted to 4-h periods. Wing discs were

dissected at 144–148 h after egg laying (AEL). For pupal wing dissections, prepupae were collected and pupal wing dissections performed the following day at 24 h after puparium formation (APF).

For wing disc immunofluorescence, discs were dissected in ice-cold phosphate-buffered saline (PBS). Isolated discs were fixed in 4% paraformaldehyde in PBS for 30 min, washed with PBS twice for 5 min each time, and then permeabilized in 0.3% Triton X-100 for 15 min. Discs were then washed in PBS twice for 5 min each time before being blocked in blocking buffer (3% bovine serum albumin [BSA], 5% goat serum, 0.1% saponin in PBS) for 1 h at room temperature. After blocking, discs were incubated in the primary antibody solution diluted in blocking buffer overnight at 4°C. Discs were washed in 0.1% saponin in PBS four times for 10 min each wash before being incubated in secondary antibody for 2 h at room temperature. Discs were then washed again in 0.1% saponin in PBS four times for 10 min each time. Finally, discs were mounted in Vectasheild mounting medium (Vector Labs). *Stim RNAi*, *Orai RNAi*, and *Best2 RNAi* immunostained wing discs were imaged using a histology microscope (eclipse 80I; Nikon) and *SERCA RNAi* immunostained wing discs were imaged using a confocal microscope (Zeiss LSM 780).

Immunofluorescence of p-Mad-stained wing discs was quantified by taking line scans perpendicular to the A/P boundary just dorsal of the D/V boundary. Five line scans were taken for each wing disc and values averaged to get an average fluorescence profile for each wing disc. The minimum fluorescence value in each average fluorescence profile was used as the background fluorescence value and was subtracted to normalize the fluorescence profiles. Maximum fluorescence values from each average fluorescence profile were used to compare the max p-Mad fluorescence between control and experimental wing discs, and *t*-tests or Mann–Whitney *U* tests were used for statistical analysis.

For pupal wing immunofluorescence the pupal cases of 24 APF pupae were removed, and the naked pupae were then fixed in 4% paraformaldehyde in PBS overnight. Wings were isolated and cuticle removed in ice-cold PBS and then permeabilized in 0.3% Triton X-100 for 15 min. Pupal wings were then washed in PBS twice for 5 min each time before being blocked in blocking buffer (3% BSA, 5% goat serum, 0.1% saponin in PBS) for 1 h at room temperature. After blocking, pupal wings were incubated in the primary antibody solution diluted in blocking buffer overnight at 4°C. The pupal wings were washed in 0.1% saponin in PBS four times for 10 min each wash before being incubated in secondary antibody for 2 h at room temperature. The pupal wings were then washed again in 0.1% saponin in PBS four times for 10 min each time. Finally, the pupal wings were mounted in Vectashield mounting medium (Vector Labs).

Primary antibodies used include rabbit anti-p-Mad (1:100 dilution, Catalog No. 9516; Cell Signaling Phospho-Smad1/5 [Ser463/465] [41D10] Rabbit mAb) and mouse anti-wingless (Wg) (1:20 dilution, Catalog No. 4d4; Developmental Studies Hybridoma Bank). Secondary antibodies include Alexa Fluor 594 goat anti-rabbit immunoglobulin (Ig) G (1:700 dilution; Invitrogen) and Alexa Fluor 488 goat anti-mouse IgG (1:700 dilution; Invitrogen).

GCaMP imaging

For larval wing disc GCaMP imaging, wing imaginal discs from 144 to 148 h AEL *MS1096-gal4>GCaMP7s* third instar larvae were dissected in HL3.1 saline solution (70 mM NaCl, 5 mM KCl, 1.5 mM $CaCl_2$, 4 mM $MgCl_2$, 10 mM $NaHCO_3$, 5 mM trehalose, 115 mM sucrose, and 5 mM HEPES, pH7.4).[56] Discs were placed on slides in HL3.1 saline between two pieces of double-sided tape to prevent crushing of the disc under the coverslip. The peripodial membrane of the wing discs faced the coverslip. The discs were then imaged using a 488 nm laser on a confocal laser scanning microscope (Zeiss LSM 780) at 2 Hz for 4 min.

For assessment of impact of thapsigargin treatment on wing disc calcium activity, *MS1096-gal4>GCaMP7s* wing discs were prepared and imaged as described previously, but mounted in HL3.1 with 25 μM thapsigargin in dimethyl sulfoxide (DMSO). Control wing discs were mounted in HL3.1 with the equivalent volume of DMSO. Regions of interest with highest variance that were 10 pixels wide to include only one cell per region of interest (ROI) were selected for analysis. Five cells per wing disc were analyzed. The fluorescence profile for the region of interest was measured and plotted over time, and the maximum and minimum GCaMP fluorescence for each ROI was used to calculate the amplitude of calcium oscillations. The average amplitude of GCaMP oscillations in control (DMSO-treated) and thapsigargin-treated wing discs were compared using *t*-tests.

For pupal wing GCaMP imaging, *dpp-gal4>GCaMP7s* prepupae were selected 24 h before imaging. At 24 h APF, the pupal cases were removed from the pupae, and pupae were mounted on slides in HL3.1 saline solution,[56] between double-sided tape to prevent crushing and with wings facing the coverslip. The wings were then imaged using a 488 nm laser on a confocal laser scanning microscope (Zeiss LSM 780) at 2 Hz for 5 min. Cells with the highest variance were selected as regions of interest. The fluorescence profile for the region of interest was measured and plotted over time, and the maximum and minimum GCaMP fluorescence in each fluorescence profile was used to calculate oscillation amplitude.

Dpp-GFP secretion imaging

For larval wing discs an endogenous green fluorescent protein tagged to Dpp (Dpp-GFP) was used for imaging of wing imaginal discs as previously described.[57] Wing discs from 144 to 148 h AEL *dpp-gal4 > dpp-GFP* third instar larvae were dissected in HL3.1 saline solution (70 mM NaCl, 5 mM KCl, 1.5 mM $CaCl_2$, 4 mM $MgCl_2$, 10 mM $NaHCO_3$, 5 mM trehalose, 115 mM sucrose, and 5 mM HEPES, pH7.4).[56] Discs were placed on slides in HL3.1 saline containing either 25 μM thapsigargin in DMSO or the control volume of DMSO between two pieces of double-sided tape to prevent crushing of the disc under the coverslip. The peripodial membrane of the wing discs faced the coverslip. The discs were then imaged using a 488 nm laser on a confocal laser scanning microscope (Zeiss LSM 780) at 2 Hz for 4 min. Images were collected for analysis at both 5 and 15 min after wing discs were dissected and placed in media with thapsigargin or control DMSO.

To analyze Dpp-GFP secretion, rectangular regions of interest that were 75 pixels wide and 215 pixels high were

selected on the dorsal side of the Dpp-GFP secreting cells just ventral to the D/V boundary. The visible D/V boundary was used as a landmark to ensure analogous regions of interest were selected from each wing disc. Within each larger regions of interest fluorescent Dpp-GFP secretion events were quantified to compare Dpp-GFP secretion event numbers between control (DMSO-treated) and thapsigargin-treated wing discs. Four-pixel wide fluorescence profiles were taken of each Dpp-GFP secretion event and the maximum and minimum fluorescence values used to calculate Dpp-GFP secretion event amplitude. Mann–Whitney *U* statistical tests were used for comparisons between control and thapsigargin-treated wing discs.

Calculations of area under the curve

Background subtracted fluorescence values from the average of three line scans per wing disc in each condition were transformed into R data frames using standard R packages [2–5]. Data frames consist of a column representing relative distance, in micrometers, from the start of the line scan, as x. There is one column per wing disc per condition containing fluorescence values that is designated y in all calculations. The (area under the curve) auc()function from the Miscellaneous Esoteric Statistical Scripts [1] package in R was used to calculate auc values as auc(x, y, from = 0, type = ''linear'') using linear interpolation. We further optimized the auc() function by adjusting the subdivisions argument in positive increments of 1000 to auc(x, y, from = 0, type = ''linear,'' subdivisions = 1000).

We performed absolute and nonabsolute calculations for each dataset by setting the auc() function argument ''absolutearea'' to TRUE and FALSE, respectively. To separate the auc value of peak 1 from the auc value of peak 2, cutoff values were manually determined and added into the auc() function. To get peak 1 auc values, the auc() function ''from'' argument was set to 0 and the ''to'' argument was assigned as the peak 1, auc(x, y, from = peak 1 cutoff, type = ''linear,'' subdivisions = 1000). To get peak 2 auc values, the ''from'' argument was assigned as the peak 1 cutoff auc(x, y, from = peak 1 cutoff, type = ''linear,'' subdivisions = 1000). All auc values were concatenated into an array and exported as .csv files that were transferred to GraphPad PRISM for visualization and statistical analysis. All code, output, and input data are found in a Git repository at https://github.com/jrb07/auc_bates.git

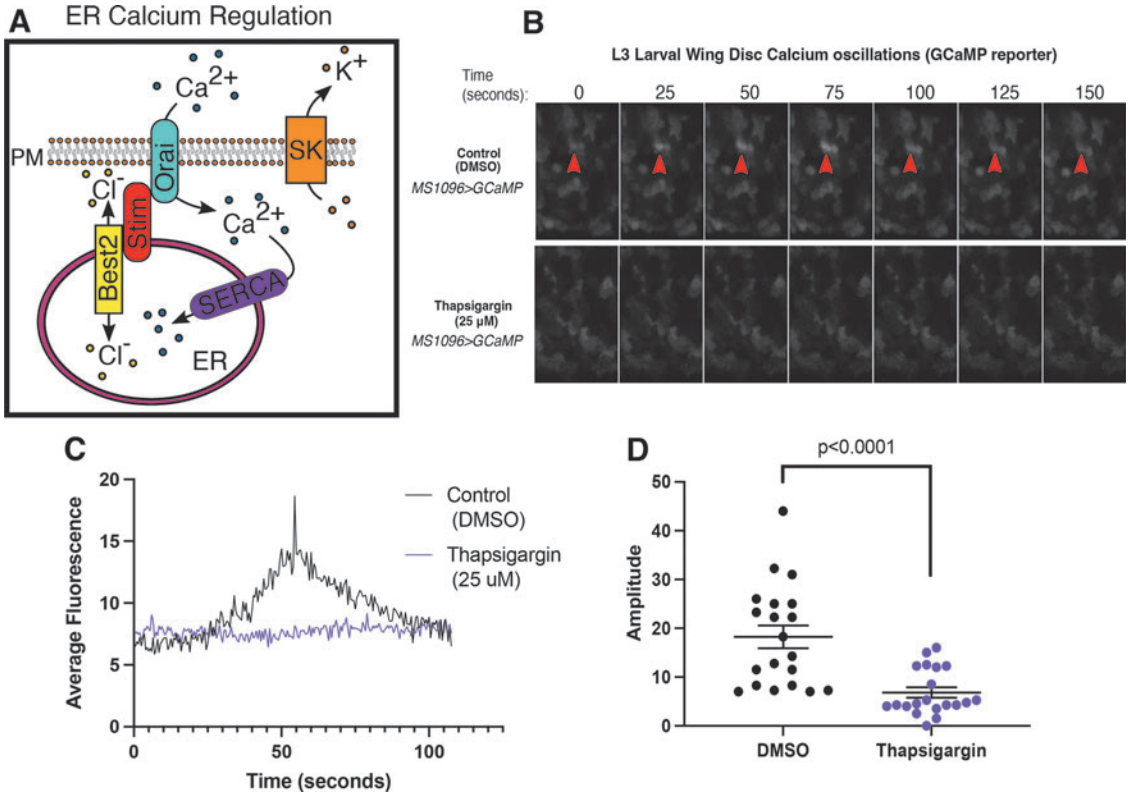

FIG. 1. Endogenous transient changes in cytoplasmic calcium are mediated by ER calcium stores. **(A)** A schematic shows how five proteins work together to mediate ER calcium stores. SERCA pumps cytoplasmic calcium into the ER. Ion channels like bestrophins act as counterbalances to maintain membrane potential by passively allowing chloride to move into and out of the ER. Stim senses calcium levels in the ER and works with Orai to open to allow extracellular calcium to pass into the cytoplasm. SK is a potassium channel that works as a counterbalance to Orai, letting potassium out of the cytoplasm. **(B)** Sequential images of GCaMP fluorescence show transient changes in cytoplasmic calcium in an MS1096>GCaMP wing control (top) and with SERCA inhibition with thapsigargin (bottom row). **(C)** Quantification of GCaMP fluorescence changes over time in MS1096>GCaMP control (DMSO, black) and thapsigargin (purple) show reduced amplitude of changes in fluorescence. **(D)** Amplitudes of individual changes in GCaMP fluorescence are compared in DMSO control (black) and thapsigargin (purple) treated larval wing discs. DMSO, dimethyl sulfoxide; ER, endoplasmic reticulum; PM, plasma membrane; SERCA, sarcoEndoplasmic reticulum calcium ATPase; SK, small conductance calcium-activated potassium channel.

Results

Inhibition of SERCA disrupts spontaneous calcium oscillations in third instar larval wing discs

Cells in the *Drosophila* third instar larval wing disc undergo spontaneous calcium oscillations (transients).[40,42–46] To determine if ER calcium contributes to larval wing disc calcium transients, we expressed the calcium indicator GCaMP7s in the developing wing using the *MS1096-gal4* driver and live imaged fluorescence with and without treatment with thapsigargin, a SERCA inhibitor. Untreated *MS1096-gal; UAS GCaMP* larval wing discs exhibit spontaneous calcium oscillations with an average amplitude of 18.2 ± 12.33 arbitrary units (Fig. 1B–D, $n = 3$) across the entire GCaMP expressing region (wing disc pouch). Inhibition of SERCA reduces the amplitude of calcium transients (6.8 ± 1.06 AU, $n = 20$, $p < 0.0001$, *t*-test, Fig. 1B–D).

Calcium transients were abundant in control wing discs such that we easily identified and quantified attributes of 87 different calcium transients. Thapsigargin treatment reduced the number of calcium transients such that only six transients could be identified in all treated discs ($n = 4$ discs). This suggests that the spontaneous calcium oscillations that occur in the developing larval wing disc require SERCA function, indicating that the calcium oscillations are mediated by ER calcium.

Spontaneous calcium oscillations occur in the developing pupal wing

To determine if cells in pupal wings undergo transient changes in cytoplasmic calcium, we expressed GCaMP in the wing using the MS1096 driver, removed the pupal case 24 h APF, and live imaged the wing. We found dynamic changes in GCaMP fluorescence in pupal wing cells. Like in the wing disc, transient changes in calcium could occur in individual cells, independent of neighboring cells (Fig. 2A, top row; Supplementary Video S1). Pupal wing calcium oscillations occur periodically at an average frequency of 2.6 ± 0.14 peaks per cell per 5 min (Fig. 2A, top row, $n = 8$ pupal wings). Alternatively, calcium transients in the pupal wing could be part of calcium waves—moving across the wing tissue (Supplementary Video S2), or fluttering within single cells (Supplementary Video S3). Pupal wing calcium oscillations have an average amplitude of 16.4 ± 12.9 AU (Fig. 2C, $n = 8$ pupal wings, and 84 cells [ROIs]). Calcium oscillations were observed in all regions of the pupal wing examined including near the wing hinge, along the wing edge and wing tip, in the intervein regions, and in the pro-vein regions.

Knockdowns of Stim and SERCA disrupt spontaneous calcium oscillations in the pupal wing

To determine if ER calcium contributes to pupal wing calcium oscillations, we expressed *stim* or SERCA RNAi along with GCaMP7s with a wing-specific *MS1096-gal4* driver. Quantitative reverse transcription polymerase chain reaction (RT-PCR) showed that RNAi significantly reduced expression of *SERCA* and *Stim* (Fig. 2E). We live-imaged pupal wings 24 h APF measuring fluorescence of GCaMP twice per second over 5 min. Wild-type pupal wing cells underwent calcium transients at a frequency of 2.64 ± 0.14 per 5 min.

The number of recorded calcium events per 5 min was reduced by knockdown of Stim (0.71 ± 1.13, $p < 0.0001$, *t*-test) compared with the wild type (Fig. 2A, middle row, B). *SERCA* RNAi almost completely ablated calcium events, such that only two events were recorded across all *SERCA* RNAi pupal wings (Fig. 2A, bottom row, B). The average amplitude of the calcium events in wild-type pupal wings was 16.41 ± 0.86 AU. Stim RNAi and SERCA RNAi significantly reduced the amplitude of the calcium oscillations (8.75 ± 1.13 AU Stim RNAi, $p < 0.0001$, *t*-test and SERCA RNAi 4.94 ± 0.53 AU, $p < 0.0001$, *t*-test, respectively; Fig. 2C; Supplementary Videos S4 and S5). Stim RNAi knockdowns decrease duration of calcium transients ($55 \text{ s} \pm 36.5$ ms, $p = 0.033$, *t*-test) compared with the wild type ($68.9 \text{ s} \pm 34$ ms) (Fig. 2D). Both Stim and SERCA RNAi significantly reduced baseline cytoplasmic calcium levels (46.9 ± 3 AU wild type, 15.3 ± 1.9 AU Stim RNAi, and 12.1 ± 1.3 AU SERCA RNAi, $p < 0.0001$, Kruskal–Wallis test; Fig. 2F) measured by GCaMP7s fluorescence within the first frame of each video taken. Together, these data show that pupal wings display endogenous calcium transients that are mediated by ER calcium channels Stim and SERCA.

ER calcium regulatory channels are required for Drosophila *wing development*

How calcium oscillations contribute to development and molecular signaling cascades is largely unknown. To test the hypothesis that calcium oscillations contribute to *D. melanogaster* wing development, we reduced the function of five ER calcium regulatory proteins (SERCA, Stim, Orai, SK, and Best2) specifically in the developing wing and assessed wing morphology. We used three different wing-specific gal4 drivers (*MS1096-gal4*, *nub-gal4*, and *Dpp-gal4*) to drive RNAi expression and knockdown each channel in the developing wing. These three drivers express in both the developing larval wing disc and the pupal wing within slightly different regions (Supplementary Fig. S1).

Nub-gal4 and *MS10960-gal4* are expressed throughout the wing disc pouch during the larval stage, with *MS1096-gal4* having slightly lower expression levels. At the pupal wing stage, *nub-gal4* becomes restricted to the vein regions, whereas *MS1096-gal4* maintains a broader expression level throughout the wing blade making it possible to compare different RNAi expression localization on phenotypes at the pupal stage (Supplementary Fig. S1). *dpp-gal4* is a useful driver for investigating potential cell autonomous effects on BMP/Dpp signaling because it expresses along the A/P border specifically within the BMP/Dpp producing cells of both the wing disc and the pupal wing and does not express broadly throughout the developing wing.

Expression of mCherry RNAi driven by each of the three gal4 drivers results in normal wing formation (Fig. 3, top row). Wing-specific knockdown of any of the five channels gives rise to severe wing defects, suggesting that ER calcium regulation is central to proper wing development in *Drosophila* (Fig. 3). Quantitative PCR confirmed reduced expression of each gene (Supplementary Fig. S2). The wing phenotypes that occur upon knockdown of ER regulatory proteins can be grouped into two categories: thickened veins and loss of veins. Stim and Orai, which function together to bring calcium into the cytoplasm, cause nearly identical

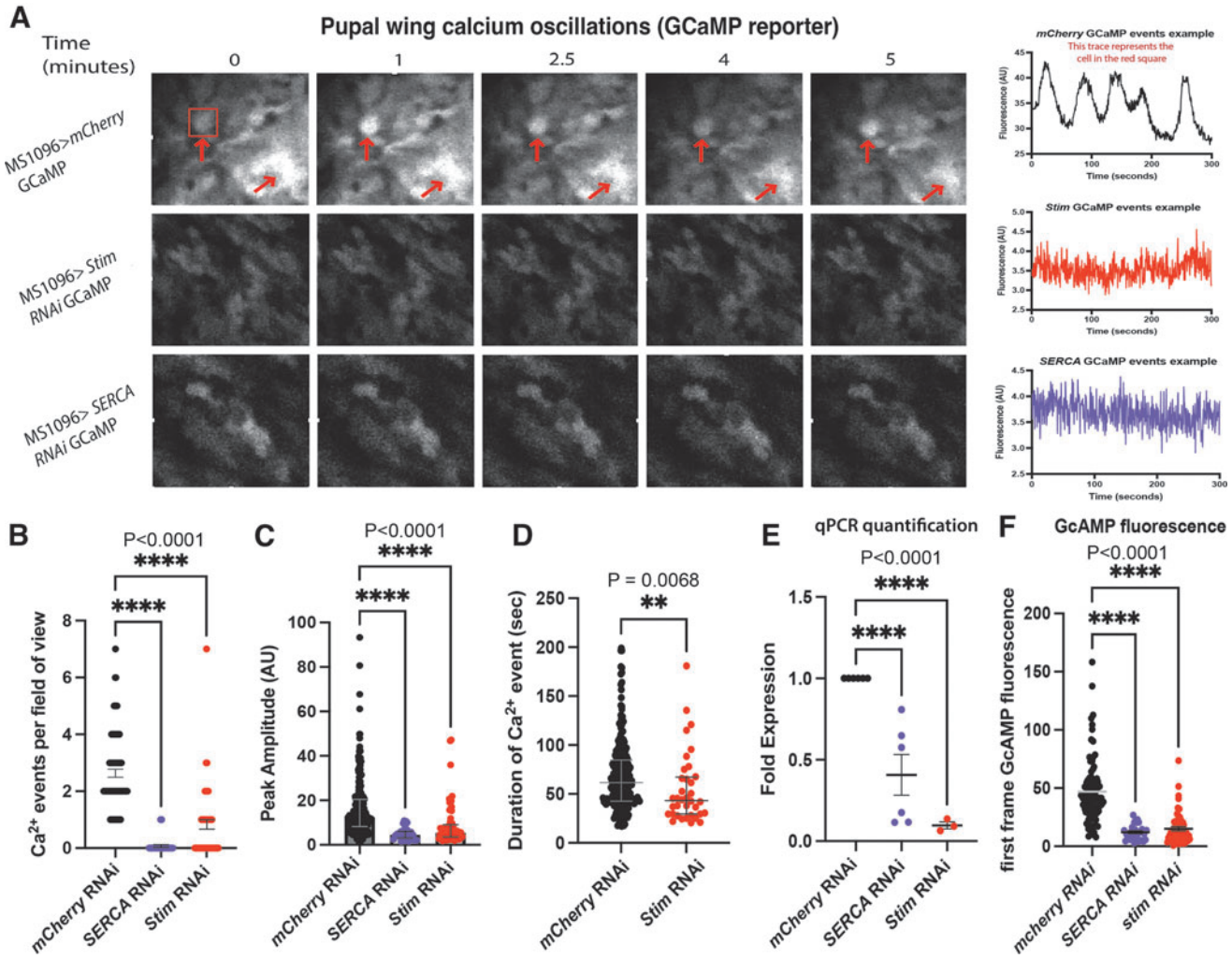

FIG. 2. Pupal wings have endogenous transient changes in cytoplasmic calcium that are mediated by ER calcium. **(A)** Representative sequential images (left) and fluorescence profiles (right) of GCaMP fluorescence in pupal wings in MS1096> GCaMP (top panels), MS1096>GCaMP; Stim RNAi (middle panels), MS1096>GCaMP; SERCA RNAi (bottom panels) show that reducing Stim and SERCA expression reduce calcium transients. **(B)** Quantification of calcium events per field of view out of seven possible shows reduced number of calcium events with *SERCA* and *stim* RNAi. **(C)** Quantification of GCaMP fluorescence peak amplitude shows that SERCA and stim RNAi reduces GCaMP fluorescence peak amplitude. **(D)** Duration of calcium events is reduced with *stim* RNAi. **(E)** Quantitative RT-PCR shows that RNAi knockdown of *SERCA* and *stim* reduced expression of each gene. **(F)** GCaMP fluorescence values of the first frame in each video used for analysis. Shown is every ROI taken from each genotype, to compare relative GCaMP (calcium) expression after knockdown. ROI, region of interest; RT-PCR, reverse transcription polymerase chain reaction.

phenotypes with each driver. Knockdown of Orai or Stim in the wing pouch of the larval wing disc and the blade of the pupal wing using either the *MS1096-gal4* or *nub-gal4* drivers results in thickening of the wing veins and a reduction in overall wing size (Fig. 3A, C, D). Reduction of Stim and Orai function RNAi expression using the *nub-gal4* driver produces slightly more severe phenotypes (Fig. 3A, C, D). Thickening of the wing veins occurs with disruption in pupal BMP/Dpp or Notch signaling, suggesting that ER calcium may be important for Notch or BMP/Dpp signaling.[58,59]

Knockdown of SK and Best2, potassium and chloride channels that counterbalance calcium flux across either the plasma membrane or the ER membrane (Fig. 1A) result in a reduction of wing size and a complete loss of veins (Fig. 3A, E, F). Knockdown of SERCA dramatically reduces wing size (Fig. 4). The reduction in wing size upon knockdown of SERCA, SK, or Best2 occurs in both the anterior and posterior compartments and suggests either cell death, reduced proliferation, or a loss of wing blade growth.

Reducing function of ER calcium regulatory proteins with RNAi *Dpp-gal4* limits the phenotypes to the region of expression, near the third longitudinal vein (L3) (Fig. 3, right column). *Dpp-gal4*-driven Orai RNAi, Stim RNAi, and SERCA RNAi results in thickening of L3 while also reducing the L3/L4 intervein region (Fig. 3, right column). *Dpp-gal4* driven SK RNAi or Best2 RNAi disrupts formation of the anterior cross vein and reduces the L3/L4 intervein region size (Fig. 3E, F). The L3/L4 intervein region spacing is

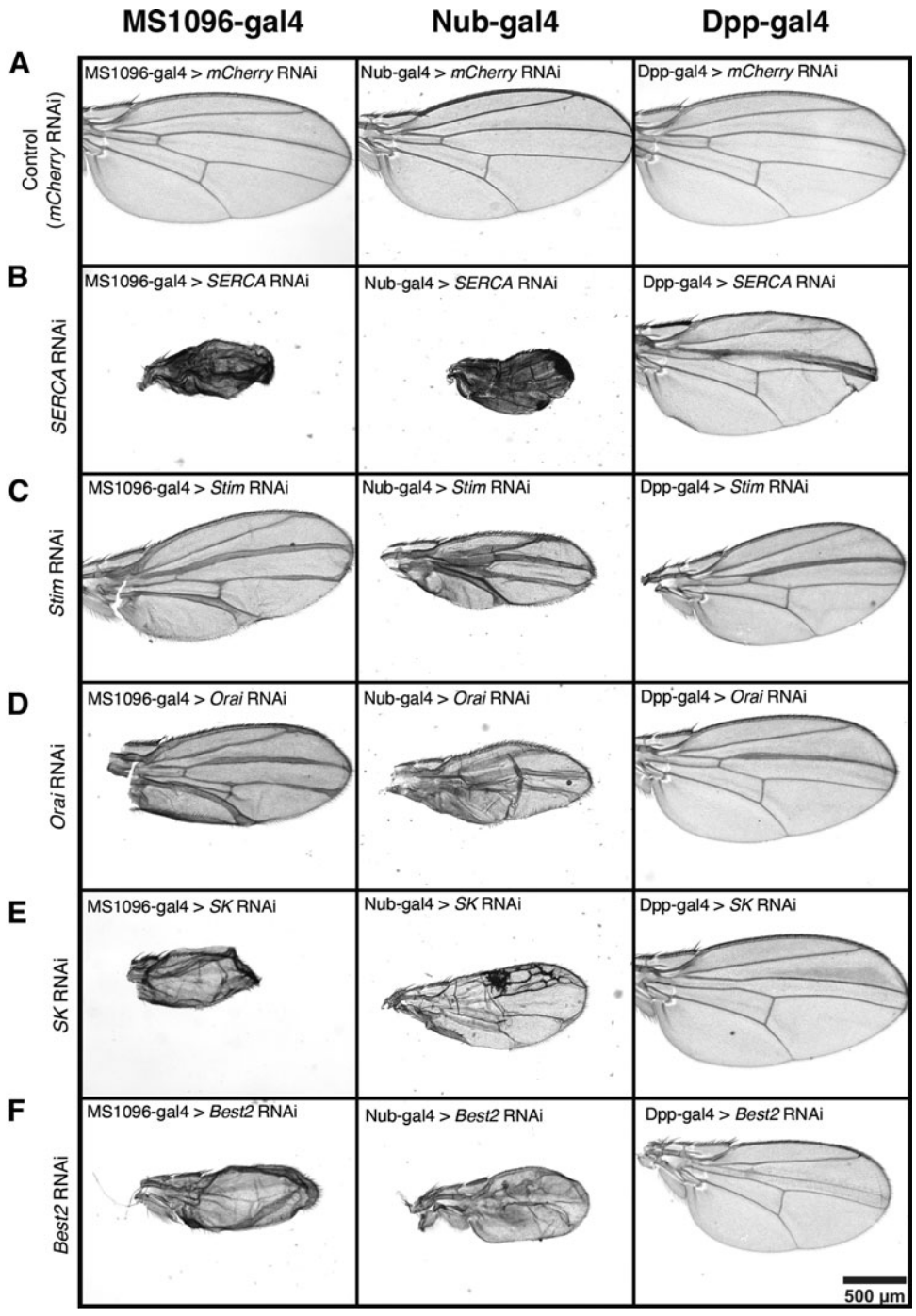

FIG. 3. Wing-specific knockdown of SERCA, Stim, Orai, SK, and Best2 have severe wing phenotypes. **(A)** Representative images of female adult wings from *MS1096>mcherryRNAi* (left), *nub>mcherryRNAi* (middle); *dpp>mcherryRNAi* (right) are controls for effects of driver lines. **(B)** Representative images show female adult wings from *MS1096> SERCA RNAi* (left) and *nub>SERCA RNAi* (middle) *dpp>SERCA RNAi* (right) are reduced in size, have bristle patterning defects, and disrupted venation. **(C)** Representative images show female adult wings from *MS1096> stim RNAi* (left) and *nub>stim RNAi* (middle) *dpp>stim RNAi* (right) have thickened veins and are reduced in size. **(D)** Representative images show female adult wings from *MS1096>orai RNAi* (left) and *nub>orai RNAi* (middle) *dpp>orai RNAi* (right) have thickened veins and are reduced in size. **(E)** Representative images show female adult wings from *MS1096>SK RNAi* (left) completely lack venation and are reduced in size. *nub>SK RNAi* (middle) have disrupted venation pattern and are reduced in size. *dpp>SK RNAi* (right) are slightly reduced in size and lack the anterior cross vein. **(F)** Representative images show female adult wings from *MS1096>best2 RNAi* (left) and *nub>best2 RNAi* (middle) completely lack venation and are reduced in size. *dpp>best2 RNAi* (right) are slightly reduced in size and lack the anterior cross vein.

FIG. 4. Phosphorylation of Mad is altered with the loss of Stim and Best2. **(A)** A representative image of a *MS1096>mcherryRNAi* shows a wild-type pattern of p-Mad staining for control. **(B)** A representative trace of fluorescence across the wing disc from anterior to posterior shows anterior (first peak) and posterior peak fluorescence (second peak) and area under the curve. A representative image of *MS1096>Stim RNAi* shows an increase in p-Mad fluorescence **(C)**, a trend toward an increase in peak fluorescence for anterior peaks and a significant increase in fluorescence of posterior peaks **(D, E)**, and an increase in area under the curve **(F)**. A representative image of a wing disc expressing *orai RNAi* **(G)** shows a trend toward an increase in average fluorescence anterior and posterior peak fluorescence and area under the curve that is not significant **(H–J)**. A representative image of a p-Mad stained *MS1096>SERCA RNAi* (K) wing disc is not significantly different from controls **(L–N)**. A representative image of *MS1096>Best2 RNAi* shows a significant decrease in p-Mad staining fluorescence area under the curve **(P)** and a trend toward a decrease in peak fluorescence **(Q, R)**.

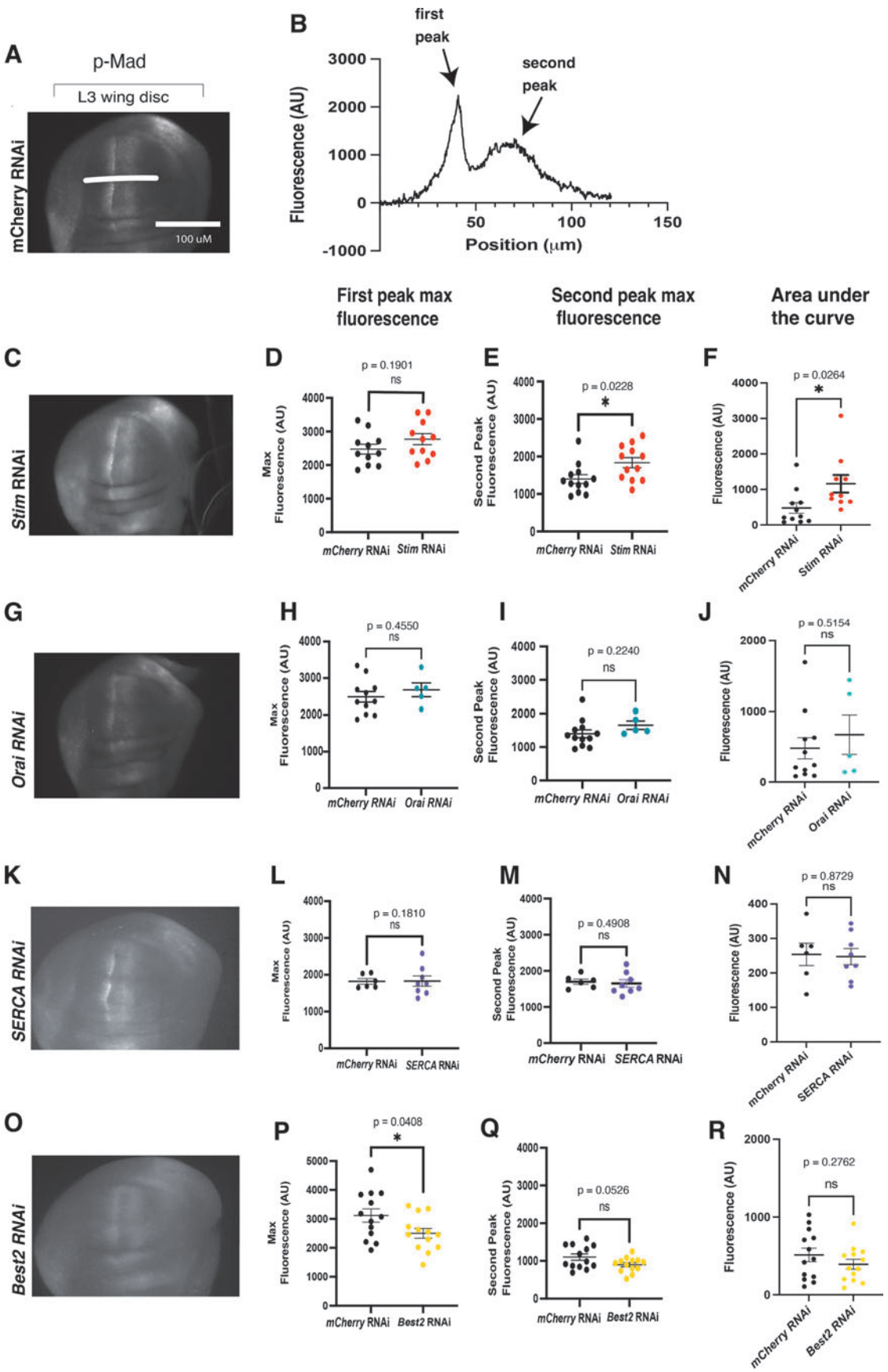
A
p-Mad
L3 wing disc
mCherry RNAi
100 uM
B
first peak
second peak
Fluorescence (AU)
Position (μm)
First peak max fluorescence
Second peak max fluorescence
Area under the curve
C
Stim RNAi
D
p = 0.1901
ns
Max Fluorescence (AU)
mCherry RNAi
Stim RNAi
E
p = 0.0228
*
Second Peak Fluorescence (AU)
F
p = 0.0264
*
Fluorescence (AU)
G
Orai RNAi
H
p = 0.4550
ns
I
p = 0.2240
ns
J
p = 0.5154
ns
K
SERCA RNAi
L
p = 0.1810
ns
M
p = 0.4908
ns
N
p = 0.8729
ns
O
Best2 RNAi
P
p = 0.0408
*
Q
p = 0.0526
ns
R
p = 0.2762
ns

controlled by Hh signaling and thus a reduction in the size of this region may indicate a disruption in Hh signaling.[59] However, because reduction in L3/L4 intervein region size is not seen when the RNAi constructs are driven by *MS1096-gal4* or by *nub-gal4*, this phenotype may be more indicative of cell autonomous cell death or disruption of short range signaling.

The phenotypes that result from disrupting SERCA, Stim, Orai, SK, and Best2 phenocopy wing defects caused by disruption of the BMP/Dpp signaling and Notch signaling. Disruption of either of these pathways can cause thickening of veins or loss of veins.[59] During wing development, both Notch and BMP/Dpp signaling help maintain and refine the wing veins. BMP/Dpp is important for growth of the wing pouch during wing development and a loss of BMP/Dpp signaling can cause growth defects, leading to underdeveloped wings.[60] For each of the five RNAi constructs targeting the ER calcium regulating proteins, the adult wings showed size defects, consistent with a loss of BMP/Dpp signaling (Fig. 3).

During the early pupal stage of development BMP/Dpp signaling becomes restricted to the wing veins and is important for the final vein cell fate determination.[58,59] Loss of BMP/Dpp signaling at this stage can cause loss of vein formation similar to the phenotypes of SK or Best2 RNAi expressing wings.[58,59] Vein thickening that is seen upon expression of Stim or Orai RNAi is also consistent with an impact on BMP/Dpp signaling (Fig. 3). During the pupal stage of wing development, BMP/Dpp signaling is restricted to the wing veins by higher expression of the BMP/Dpp receptor Tkv.[58,59] Loss of Tkv expression or an increase in BMP/Dpp expression leads to a broader range of BMP/Dpp signaling, causing more cells to adopt a vein cell fate and subsequent thickening of the wing veins.[58,59]

In addition to BMP/Dpp, Notch signaling is required for vein refinement and disruption can cause vein thickening during wing development, as seen in phenotypes of orai and stim knockdown.[58,59] During development Notch ligands Delta and Serrate are expressed within the proveins while Notch is expressed in cells flanking the veins, this cellular crosstalk relies on Notch signaling to restrict vein size. In addition, overactivation of Notch signaling can lead to the loss of veins.[58,59]

Reduction in wing size, loss of venation, and vein thickening are phenotypes observed after knockout of ER calcium regulatory proteins (SERCA, Stim, Orai, SK, and Best2). These phenotypes are consistent with disruptions to developmental signaling cascades such as BMP/Dpp and Notch signaling during the larval or pupal stages.[58,61–63] The similarity of the phenotypes suggests that ER calcium regulation may be required for BMP/Dpp or Notch signaling.

ER calcium is important for developmental signaling

Disruption of BMP/Dpp or Notch signaling in the *Drosophila* wing during the larval or pupal stages can lead to loss of veins or increase in vein width and growth of ectopic veins. Previous studies in the *Drosophila* wing have found that Notch signaling is disrupted when the function of SERCA or Stim was reduced.[64,65] Following wing-specific RNAi-driven knockdown of SERCA, Stim, Orai, and Best2 we collected larval wing discs and stained for Wg, a downstream transcriptional target of the Notch pathway.[63] We found that *wg* was expressed as expected near the D/V boundary when SERCA ($n=11$), Stim ($n=4$), Orai ($n=4$), or Best2 ($n=13$) were knocked down (Supplementary Fig. S3). Only Best2 RNAi caused a minor decrease in *Wg* expression on the anterior side of the pouch (Supplementary Fig. S2; $n=13$). Eid et al. found that *wg* expression in the larval wing disc was impacted by overexpression of Stim.[64] We did not find a similar impact on *wg* expression upon knockdown of Stim (Supplementary Fig. S3). These results suggest that these ER calcium regulatory proteins are not required for Notch signaling during the third instar larval stage.

We previously found that ion channel function is important for BMP/Dpp signaling in the *Drosophila* larval wing.[12,20,40] To determine how ER calcium regulation affects BMP/Dpp signaling we knocked down SERCA, Stim, Orai, or Best2 and measured phosphorylated Mad (p-Mad), a downstream effector of BMP/Dpp, using immunofluorescence (Fig. 4). In control larval wing discs expressing wing-specific mCherry RNAi, p-Mad can primarily be found on either side of the anterior/posterior boundary in the wing disc pouch (Fig. 4A). This pattern is not disrupted by RNAi reducing expression of SERCA, Stim, Orai, or Best2 in the wing disc (Fig. 4—representative images). To determine whether BMP/Dpp signaling pathway was impacted in a more subtle manner at the larval stage, p-Mad fluorescence was quantified using line scans across the wing disc pouch dorsally to the D/V boundary (example line scan shown in Fig. 4A, B—quantifications and graphs).

Expression Stim RNAi ($n=11$) significantly increases the posterior peak fluorescence (Fig. 4E), and the AUC of p-Mad fluorescence (Fig. 4F). Expression of Orai RNAi ($n=5$) trends toward an increase in the AUC of p-Mad fluorescence (Fig. 4J). Wing-specific expression of SERCA RNAi ($n=8$) does not significantly change p-Mad fluorescence (Fig. 4L–N). Best2 RNAi causes a slight but significant decrease in peak p-Mad fluorescence intensity and a trend toward decreased AUC of p-Mad fluorescence (Fig. 4P–R, $n=13$, $p=0.0408$, *t*-test). Together, these results indicate that reducing function of Stim increases BMP/Dpp signaling and increases thickness of wing veins, whereas reducing Best2 function slightly decreases BMP/Dpp signaling in the larval wing disc and reduces venation in the wing.

We investigated whether ER calcium regulation impacts BMP signaling at the pupal stage of wing development. During this stage, BMP/Dpp signaling becomes restricted to the presumptive wing veins (Fig. 5A) and specifies wing vein differentiation.[58] At the pupal stage we found a dramatic change in p-Mad fluorescence upon knockdown of each of the ER calcium regulating proteins. Knockdown of SERCA, Stim, or Orai results in thickening of the p-Mad stripes along the presumptive wing veins (Fig. 5B–E) compared with the control wings (Fig. 5B). This increase in p-Mad thickness may indicate an expansion of BMP/Dpp signaling leading to the wing vein thickening that occurs when Stim or Orai is knocked down and the excess of vein tissue that occurs upon SERCA knockdown (Fig. 5B–E).

Best2 RNAi also disrupts p-Mad at the pupal wing stage, with immunostaining for p-Mad appearing diffusely across the entire wing rather than being restricted to the presumptive veins (Fig. 5F). Even in the early pupal stage, Best2 RNAi expressing wings have developmental defects resulting in pupal wings that are wrinkled and folded. Therefore, it is difficult to determine whether this increase in p-Mad

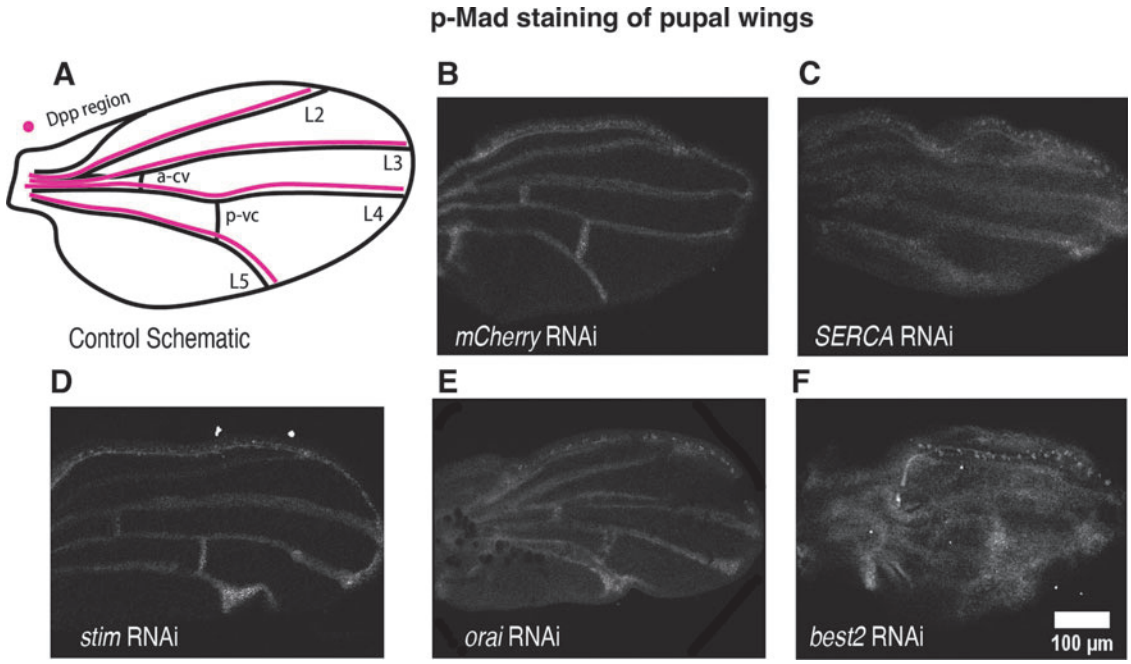

FIG. 5. Representative images of p-Mad stained pupal wings show that knockdown of ER calcium regulatory proteins disrupts BMP signaling in the pupal wing. **(A)** A schematic shows where Dpp signaling specifies wing veins **(B)** *MS1096>mCherry* RNAi pupal wings serve as controls. **(C)** *MS1096>SERCA* RNAi pupal wings have increased thickness of p-Mad staining along longitudinal veins but reduced p-Mad staining in cross veins. **(D)** *MS1096>stim RNAi* pupal wings have increased p-Mad staining. **(E)** A representative image shows *MS1096>Orai RNAi* increased the domain of p-Mad staining in pupal wings. **(F)** A representative image shows disruption of p-Mad staining in *MS1096>best2 RNAi* adult wings. BMP, bone morphogenetic protein.

immunofluorescence in Best2 RNAi expressing pupal wings is owing to an increase in Mad phosphorylation or because of nonspecific staining of antibody caught in the damaged wing tissue. Adult *MS1096-gal4>Best2 RNAi* wings show a loss of veins (Fig. 3F), which is more consistent with a loss of Mad phosphorylation. Together, these results suggest that loss of ER calcium regulation results in aberrant BMP/Dpp signaling, most noticeably in the pupal wings.

Chemical inhibition of SERCA disrupts BMP/Dpp secretion

To investigate if the ER calcium channels and cellular calcium oscillations are required for BMP/Dpp secretion within the developing wing, we treated *Dpp-GFP* expressing wing discs with μM thapsigargin, a concentration that abolished the calcium oscillations (Fig. 1) and used live imaging to examine Dpp-GFP secretion dynamics using a method developed in our laboratory.[57] We imaged the center of the wing disc pouch where Dpp-GFP is strongly expressed at a rate of two frames per second for 4 min. Regions of interest were chosen using the visible D/V boundary as a landmark (Fig. 6A, red arrowhead).

In control wing discs treated with only DMSO, Dpp-GFP secretion can be seen as bright GFP puncta close to the Dpp releasing cells (Fig. 6A, white arrow). Quantification of small regions of interest just outside the Dpp-GFP region of the wing disc show discrete rises in Dpp-GFP fluorescence consistent with Dpp-GFP secretion (example trace, Fig. 6C). In wing discs treated with thapsigargin, fewer discrete rises in Dpp-GFP fluorescence can be seen, suggesting that SERCA function is required for proper Dpp-GFP secretion (Fig. 6D, example trace).

Quantification of the number of release events within matching regions of interest in control and thapsigargin-treated wing discs 5 min after wing disc dissection and treatment show a significant decrease in the number of Dpp-GFP release events upon thapsigargin treatment (6.33 ± 1.25 control vs. 2.66 ± 0.76 thapsigargin treated, Fig. 6F, $n = 6$ wing discs, $p = 0.0316$, t-test). This decrease in release events persists over time and by 15 min postwing disc dissection and treatment, thapsigargin-treated wing discs continue to have significantly fewer release events (6.20 ± 1.07 control vs. 1.40 ± 0.51 thapsigargin treated, Fig. 6G, $n = 5$ discs, $p = 0.0036$, t-test). Thapsigargin significantly decreases amplitude of Dpp-GFP release events at both the 5-min (16.36 AU ± 1.93 control $n = 6$ wing discs vs. 9.79 ± 1.56 AU, $n = 6$ thapsigargin-treated wing discs, $p = 0.024$, t-test, Fig. 6I) and 15-min treatment timepoints (control 13.44 ± 1.54 AU control $n = 5$ wing discs, vs. 7.43 ± 1.08 $n = 5$, thapsigargin-treated wing discs, $p = 0.0128$, respectively, by t-test, Fig. 6J, $n = 6$ wing discs, $p = 0.0243$, $n = 5$ wing discs, $p = 0.0128$, respectively, t-test). This reduction in amplitude suggests that thapsigargin treatment reduces the amount of Dpp-GFP that is released at each Dpp-GFP release event in addition to decreasing the number of release events. Thus, inhibition of SERCA with thapsigargin treatment abolishes spontaneous calcium oscillations in the larval wing disc and disrupts Dpp-GFP secretion.

Similarly, reducing function of Stim with RNAi knockdown (*dpp-gal4>stim RNAi; Dpp-GFP*) reduced Dpp-GFP

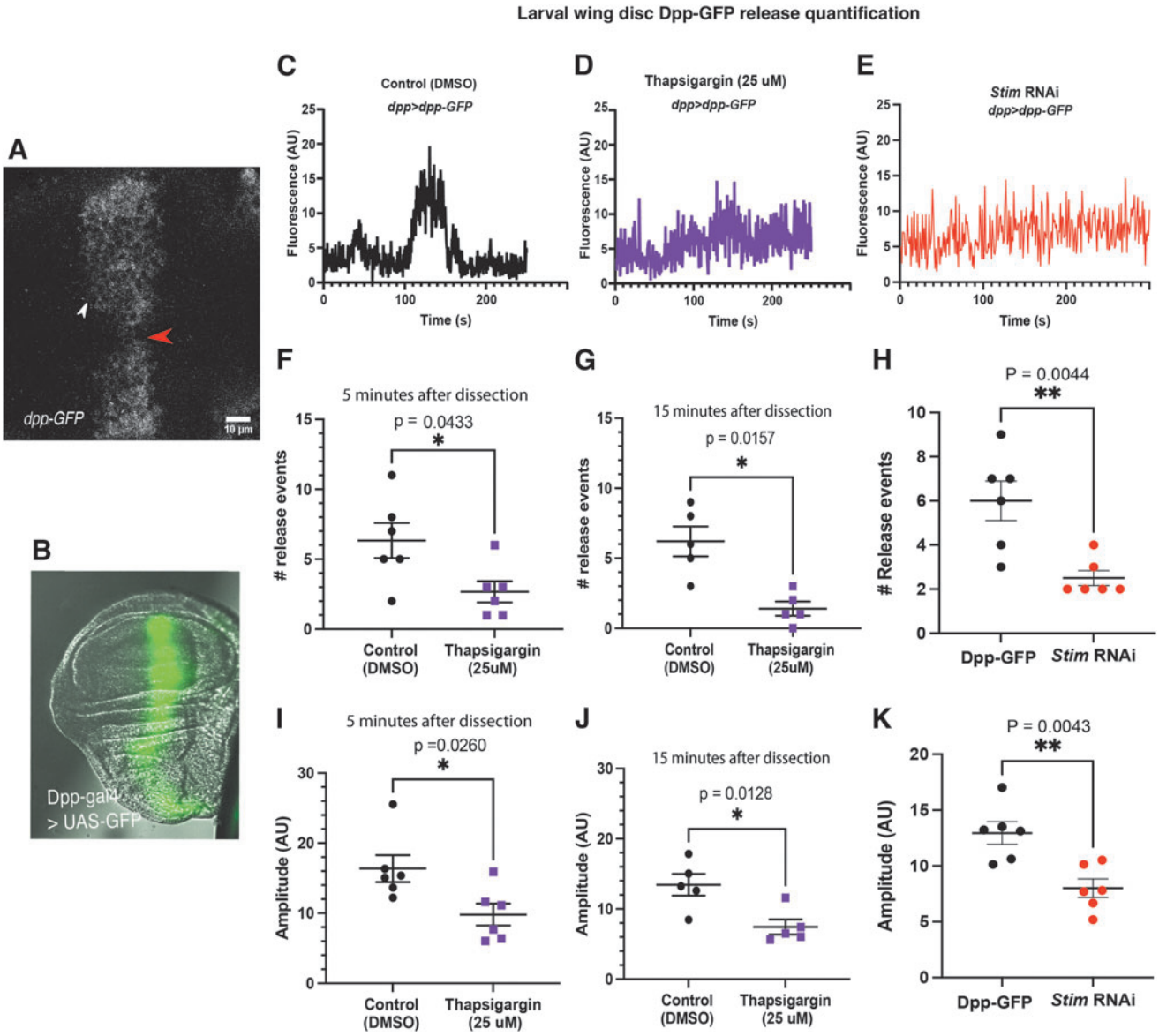

FIG. 6. Reduction of SERCA and Stim function reduces number and amplitude of Dpp-GFP release events. **(A)** A representative image of a *dpp>dpp-gfp* wing disc shows where Dpp-GFP release events were measured. **(B)** A representative image of *dpp>gfp* shows the expression zone. **(C)** A representative trace of Dpp-GFP fluorescence over time from a *dpp>dpp-gfp* wing disc shows a dramatic change in fluorescence associated with Dpp-GFP release. **(D)** A representative trace of Dpp-GFP fluorescence over time in a *dpp>dpp-gfp* incubated thapsigargin shows that SERCA inhibition reduces amplitude of Dpp-GFP fluorescence changes. **(E)** A representative trace of Dpp-GFP fluorescence over time from a *dpp>dpp-gfp;stim RNAi* wing disc shows that knockdown of Stim reduces Dpp-GFP release events. **(F, G)** Graphs show that the number of Dpp-GFP release events is significantly reduced by incubation in thapsigargin for 5 min **(F)** and 15 min **(G)**. **(H)** A graph shows that knockdown of Stim reduces the number of Dpp-GFP release events. **(I, J)** A graph shows that the amplitude of Dpp-GFP release events is reduced by incubation in thapsigargin for 5 min **(I)** and 15 min **(J)**. **(K)** A graph shows that Stim knockdown reduces the amplitude of changes in Dpp-GFP fluorescence. GFP, green fluorescent protein.

release events compared with controls (*dpp-gal4>Dpp-GFP* control 6 ± 0.89, *dpp-gal4>stimRNAi; dpp-GFP* 2.5 ± 0.34, $N = 6$, $p = 0.0044$, *t*-test; Fig. 6E, H). *Stim RNAi* reduced average amplitude of Dpp-GFP fluorescence peaks by 65% compared with control larval wing discs (*dpp-gal4>Dpp-GFP* control 12.94 ± 1.01 AU, *dpp-gal4>Stim RNAi; Dpp-GFP* 8.01 ± 0.83 AU, $N = 6$ discs, $p = 0.0036$; Fig. 6K). Dpp release events were decreased over twofold. These data support the hypothesis that ER-mediated calcium oscillations are required to maintain correctly timed BMP/Dpp secretion events.

Discussion

We show that developing *Drosophila* wings have spontaneous calcium oscillations at both the larval and pupal stages (Figs. 1 and 2). These spontaneous calcium oscillations are abolished by inhibition of SERCA and are significantly reduced by RNAi knockdown of Stim, suggesting that they are mediated by ER calcium (Figs. 1 and 2). Wing-specific disruption of five ion channels/pumps (SERCA, Stim, Orai, SK, and Best2) that regulate ER calcium and cytoplasmic

levels causes severe wing defects in *Drosophila* (Fig. 3). These severe wing phenotypes suggest that control of cytoplasmic and ER calcium is important for *Drosophila* wing development.

Disruption of SERCA, Stim, Orai, SK, and Best2 changes BMP/Dpp signaling at the larval stage (Fig. 4) and pupal stage (Fig. 5) demonstrating that ER calcium regulation is important for proper function of this signaling pathway. Disruption of calcium oscillations via inhibition of SERCA decreases BMP/Dpp-GFP secretion events and Dpp-GFP secretion event amplitude (Fig. 6). Together, these data support the hypothesis that ER calcium helps regulate spontaneous calcium oscillations and that calcium oscillations in turn regulate the secretion of BMP/Dpp (Fig. 7).

Wing-specific RNAi for SERCA, SK, and Best2 reduces wing venation, whereas disruption of Stim and Orai causes an increase in venation and vein thickness. Evidence suggests that in some contexts bestrophin chloride channels like Best2 provide a negative ion to counterbalance positive Ca^{++} pumped into the ER. Similarly, SK is a slow leak potassium channel that counterbalances positive Ca^{++} in the cytoplasm. Opposing phenotypes suggest that SERCA, SK, and Best2 counterbalance the effects of Stim and Orai on wing venation. A thickened vein phenotype can arise if SERCA, Stim, or Orai knockdown changes Notch or BMP/Dpp signaling during the pupal stage.

Our work suggests that one of the ways that each of these channels impact wing development is via alteration of BMP/Dpp signaling. Whereas SERCA knockdown reduces Dpp-GFP release events in the wing disc, it broadens the domain of Mad phosphorylation, a readout of Dpp signaling. At first glance, these results appear contradictory; however, there are multiple hypotheses that could explain these results, which we are currently exploring. One possibility is a negative feedback loop in which the cell surface localization of Dpp receptors depends upon regulated Dpp release. When the presentation of the ligand is changed, Dpp receptors are retained on the cell surface. Another possibility is that the loss of SERCA and thus change in calcium levels has a different effect on Dpp producing cells as it does on Dpp receiving cells. For example, calcium levels could potentially alter dynamics of intracellular receptor-associated endocytic vesicles to increase their signaling within the cell. These possibilities could be addressed by knocking down SERCA in clones of cells and assessing phosphorylation of Mad with an internal control.

Calcium oscillations occur throughout the pupal wing and are not strictly associated with Dpp-producing cells. Although our results suggest that ER and cytoplasmic calcium levels regulate Dpp release, our data do not address whether observed calcium oscillations are controlling other morphogen signaling. For example, SERCA, Stim, and Orai directly regulate ER calcium levels and their activity is important for regulating the cell cycle, cell polarity, and Notch signaling.[65–68] We used a previously published data single cell RNA sequencing data set[69] to identify cells that express Dpp, *SERCA,* and *stim*. SERCA and Stim are ubiquitously expressed throughout the wing disc, whereas *dpp* is only expressed in a small subset (Supplementary Fig. S4). SERCA and Stim could be mediating calcium oscillations in any of the wing disc cells.

If our hypothesis is correct, there must be an ER calcium release channel regulating calcium release from the ER into the cytoplasm. A likely candidate is the inositol triphosphate receptor (IP3R). Knockdown of IP3R disrupted calcium oscillations in the developing wing.[45] Disruption of IP3R reduces wing size and leads to a loss of the formation of the posterior crossvein (PCV[45]). Long range BMP/Dpp signaling is essential for the formation of the PCV,[70] this phenotype is consistent with a loss of BMP/Dpp signaling making IP3R a likely candidate for regulating the ER calcium release that may be necessary for regulation of BMP/Dpp secretion. Future experiments will determine if reduction in IP3R function impacts Dpp release and Mad phosphorylation in the wing disc.

Our data add to a growing body of evidence that the spontaneous calcium oscillations in a wide variety of organisms play an essential role in development. Calcium oscillations have been reported in cultures of mesenchymal stem cells,[71] chondrocytes,[72] osteoblasts,[73] keratinocytes,[74] endothelial cells,[75–77] and epithelial cells,[78–81] during early embryonic development in zebrafish,[47] *Xenopus*,[48] and mouse embryos (reviewed in Stewart and Davis[82]). Spontaneous calcium oscillations can be found in developing chick feather buds, and disruption of these oscillations leads to disrupted cellular migration and feather bud defects.[19] In blue pansy butterflies disruption of spontaneous calcium waves during pupal wing development leads to defects in wing scale development and eye spot formation.[41] Calcium oscillations have previously been reported in the larval *Drosophila* wing disc.[40,44–46]

We show that these calcium oscillations occur *in vivo* at the pupal stage of *Drosophila* wing development (Fig. 2). The presence of calcium oscillations in various developing tissues and organisms suggests that oscillations may play an overlooked role in cellular communication during development.

Regulation of ER calcium stores is required for the functioning of multiple developmental signaling pathways. Orai1, a Ca^{2+} release activated Ca^{2+} (CRAC) channel that mediates calcium entry to the cell when ER calcium stores are depleted, is required for BMP signaling in mice.[83] In humans, mutations in the genes encoding stromal interaction molecule 1 and calcium release-activated calcium channel protein 1 are associated with developmental defects including facial dysmorphism, severe dental enamel defects, and abnormalities of the skin, consistent with the evidence that these channels may regulate developmental signaling pathways.[84–86] Work carried out in human leukemia cells suggests that SERCA may be important for the Notch signaling pathway with disruption of SERCA resulting in a loss of surface accumulation of Notch.[87]

SERCA and Stim, another CRAC channel that works with Orai, are both important for proper Notch signaling in *Drosophila,* suggesting that ER calcium regulation may contribute to regulating Notch signaling in addition to BMP/Dpp.[64,88,89] Disruption of Stim in the *Drosophila* wing results in wing defects including thickening of the veins, and overexpression of Stim leads to defects in Wg signaling.[64] These defects could be rescued by expression of a constitutively active Notch allele, suggesting that Stim may play a role in Notch signaling.[64]

The ion channels we investigated are primarily involved in replenishing ER calcium stores (CRAC and store operated calcium entry-related channels) rather than the flux of calcium out of the ER. However, the IP3R, which mediates

release of calcium from the ER, is required for the propagation of calcium oscillations in the *Drosophila* wing disc.[42,44] Furthermore, wing-specific RNAi knockdown of IP3R reduces wing size, causes venation defects including incomplete posterior cross vein, and causes the wings-held out phenotype, three Dpp loss-of-function phenotypes.[53,90] Gap junctions, which mediate calcium flux between cells, are required for calcium oscillation propagation and for normal wing development.[12,19,42,44] Together, these data suggest that ER calcium stores—and the flux of calcium into and out of the ER—play an essential role in regulating the calcium oscillations that occur in developing tissues.

We show that the spontaneous calcium transients in developing tissues may regulate cell–cell communication by regulating canonical developmental signaling pathways. Using GFP-tagged Dpp to investigate BMP/Dpp secretion dynamics, we found that blocking calcium transients via inhibition of the calcium ATPase SERCA disrupts Dpp-GFP secretion (Fig. 6). This agrees with prior research from our laboratory showing that disruption of an Irk channel abolishes calcium oscillations and disrupts Dpp-GFP release.[40] In pancreatic β-cells, rises in cytoplasmic calcium induce insulin secretion.[36,91,92] In neurons, transient increases in calcium regulate the release of neurotransmitters at synapses.[93,94] The secretion of hormones in neuroendocrine cells is similarly controlled by calcium.[95–97] Changes in calcium levels also induce the exocytosis of insulin-containing secretory granules in pancreatic β cells.[98] Our results propose that a similar mechanism may be used to regulate the secretion of BMP/Dpp in the developing *Drosophila* wing.

Indeed, other similarities to the mechanisms of neurotransmitter or insulin release in excitable cells have been found in developing tissues. In neurons and pancreatic β cells, intracellular calcium activates the Soluble *N*-ethylmaleimide-Sensitive Factor Attachment Proteins (SNAP) receptor (SNARE) complex of proteins to mediate vesicle fusion and control release of signaling components.[94,99] The exocyst complex acts in cells to regulate the trafficking of vesicles to the cell's surface for SNARE-mediated fusion.[100] There is evidence that members of the SNARE and exocyst complexes also play roles in the development of non-neuronal tissues and may regulate trafficking of developmental signaling pathway components. Knockdown of Syb, a member of the SNARE complex family, or synaptotagmin-1, a calcium sensor that activates the SNARE complex, causes a disruption in BMP/Dpp signaling in the *Drosophila* ASP.[46]

In *Drosophila* ovary stem cells Sec5, Sec6, Sec10, and Sec15 are required for BMP/Dpp signaling and in *Drosophila* testis stem cells knockdown of Sec6 or Sec8 results in subsurface accumulation of Dpp.[101,102] In the *Drosophila* larval wing disc Dpp accumulated subcellularly when cells lacked Sec5 and reducing Sec5 copy number rescued lethality of Dpp overexpression.[101] These data support a model in which calcium regulates the vesicular secretion of BMP/Dpp to regulate wing development (Fig. 7).

The oscillatory nature of the calcium fluctuations that we observed as well as our observations of the dynamics of Dpp-GFP secretion suggests that BMP/Dpp may be secreted in a pulsatile manner rather than constitutively. Temporal dynamics of exposure to the BMP/Dpp-like ligand TGFβ were important for the transcriptional response of receiving cells within a stem cell culture model.[103] Pulses of ligand exposure resulted in far higher transcriptional responses and a better regulation of cell fate than constant ligand exposure.[103] This result may be owing to negative feedback loops, where a constant exposure to ligand induces a higher level of negative feedback (such as receptor internalization or inhibition) than pulsatile ligand exposure does, resulting in more pathway downregulation.[103,104] Future work comparing the dynamics of calcium oscillations and the dynamics of BMP/Dpp pulsatile secretion would help determine whether calcium oscillation drive BMP/Dpp pulses.

ER calcium inhibition might disrupt BMP/Dpp signaling because it is important for formation or maintenance of the filipodia-like cell–cell signaling structures known as cytonemes. It is possible that thapsigargin-mediated inhibition of SERCA may disrupt the formation of cytonemes that are important for signaling in the wing disc. SERCA function may be important for cytoneme formation in the ASP and that cytonemes are required for proper BMP/Dpp signaling in the ASP.[46] Thapsigargin treatment of the wing discs may similarly disrupt BMP/Dpp signaling by its effects on cytoneme formation or maintenance.

Although our work suggests that calcium oscillations are necessary for proper BMP/Dpp release, future experiments are needed to probe whether calcium is sufficient to induce BMP/Dpp release. Our experiments do not eliminate the possibility that inhibition of SERCA with thapsigargin causes cell death or protein misfolding leading to the failure of BMP/Dpp releasing cells to secrete BMP/Dpp. Thapsigargin can induce apoptosis.[105] To avoid inducing cell death, we treated wing discs with thapsigargin for only 5 min before

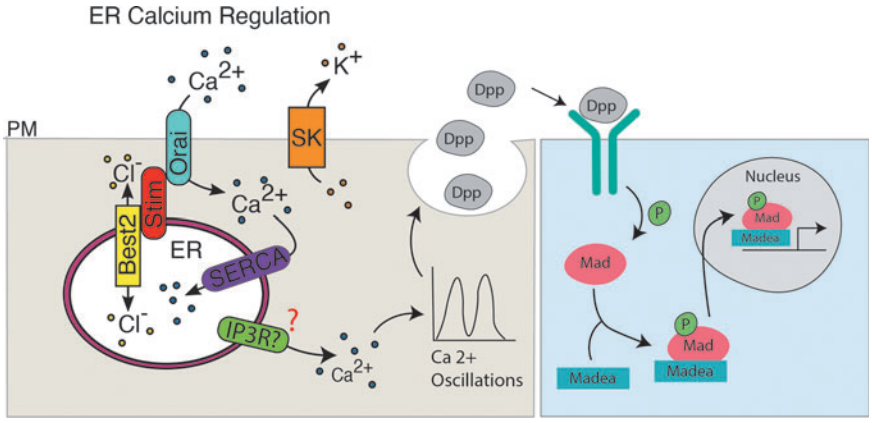

FIG. 7. Potential model for ER calcium-mediated regulation of BMP/Dpp signaling. Together SERCA, Orai, Stim, SK, and Best2 help regulate the flux of ER calcium. Calcium movement out of the ER potentially through IP3R regulates calcium oscillations that in turn regulate the fusion of BMP/Dpp containing vesicles impacting downstream signaling.

imaging Dpp-GFP secretion (see Materials and Methods section). Other studies show that cells must be exposed to thapsigargin for hours rather than minutes to induce cell death.[105,106] We saw a decrease in Dpp-GFP secretion events and fluorescence amplitude within 5 min of thapsigargin treatment, suggesting that SERCA inhibition causes BMP/Dpp secretion disruption before any potential cell death.

We tested for apoptosis in thapsigargin-treated, SERCA RNAi, or Stim RNAi wing discs and found no apoptosis in third instar wing discs in any of these conditions (Supplementary Fig. S5). Future studies looking at BMP/Dpp secretion upon induction of calcium oscillations with channel rhodopsin will be able to determine whether calcium oscillations directly induce BMP/Dpp secretion or are simply necessary to provide the conditions for BMP/Dpp secretion.

It is interesting to note that our results suggest that BMP/Dpp signaling is most disrupted at the pupal stage rather than the larval stage (Figs. 4 and 5). Owing to the technical difficulties of treating pupal wings with thapsigargin, however, we investigated the secretion dynamics of BMP/Dpp at the larval stage (Fig. 6). Although BMP/Dpp signaling is only slightly impacted at the larval stage upon expression of SERCA RNAi (Fig. 4K–N), we found a disruption of BMP/Dpp secretion dynamics upon treatment with thapsigargin at this developmental stage (Fig. 6). This difference may be owing to the very strong inhibitory impact of thapsigargin on SERCA.[107] as opposed to the potentially lessor impact of the RNAi construct on SERCA expression.

Our results also suggest that thapsigargin treatment does not entirely abolish Dpp-GFP secretion, as thapsigargin-treated wing discs still exhibit Dpp-GFP release (Fig. 6). It is possible that this decrease in Dpp-GFP secretion is not significant enough to cause large changes in downstream BMP/Dpp signaling explaining our immunohistochemistry results. Calcium oscillations in the developing wing disc are highest during early development and were reduced as the wing disc approached the late third instar stage.[45] We examined both p-Mad levels and the impact of thapsigargin on Dpp-GFP secretion at the late third instar stage, the relatively modest impacts of ER calcium channel disruption on Dpp-GFP secretion and Mad phosphorylation is consistent with the reduced calcium activity at this stage.

Future studies investigating the impact of ER calcium channel disruption on Mad phosphorylation and Dpp-GFP secretion in the wing disc at the second instar stage when calcium activity is higher will help elucidate whether BMP/Dpp signaling levels correlate with calcium activity. We observed calcium activity during the pupal stage and more dramatic impacts on BMP/Dpp signaling at this later stage (Figs. 2 and 5). Future studies investigating whether disrupting ER calcium oscillations during the pupal stage via expression of SERCA RNAi more significantly disrupts BMP/Dpp secretion will help determine whether the more severe impacts on BMP/Dpp seen at the pupal stage are owing to a greater disruption in BMP/Dpp secretion. Because ER calcium plays important roles in many cellular processes including cell death and cell cycle regulation, it is likely that the severe phenotypes seen in adult *Drosophila* wings upon expression of SERCA, Orai, Stim, SK, or Best2 RNAi are owing to the cumulative impacts of disruptions of multiple processes rather than a disruption of BMP/Dpp signaling alone.

We show that the ER calcium regulating channels are necessary for *Drosophila* wing development and help mediate spontaneous calcium oscillations in the developing wing at both the larval and pupal stages. Our results suggest that BMP/Dpp is secreted in a pulsatile manner requiring the function of SERCA and Stim. Disruption of the spontaneous calcium oscillations that occur in the larval wing via SERCA inhibition disrupts BMP/Dpp secretion, suggesting one mechanism by which ER calcium regulates development.

Authors' Contributions

L.F.G. performed experiments that generated most of the data presented and wrote the first draft of the article. M.L.F., E.F., J.R.B., and H.R.M. performed experiments and analysis that are included in main figures. J.R.B. wrote code that was used to determine area under the curve. Y.H.O. and M.L.F. performed bioinformatic analysis for gene expression of *Stim, SERCA*, and *Dpp*. M.L.F. and E.A.B. edited the article. E.A.B conceived, designed, and oversaw the experiments and obtained funding.

Author Disclosure Statement

No competing financial interests exist.

Funding Information

We are grateful for funding from the National Science Foundation 1945916 to E.A.B. which funds this project, and National Institutes of Health DE025311 to E.A.B. The majority of the results described in this article comprise the dissertation research of L.F.G., who defended her dissertation on August 31, 2021 and was awarded a PhD by the Molecular Biology Program from the University of Colorado Anschutz Medical School.

Supplementary Material

Supplementary Figure S1
Supplementary Figure S2
Supplementary Figure S3
Supplementary Figure S4
Supplementary Figure S5
Supplementary Video SV1
Supplementary Video SV2
Supplementary Video SV3
Supplementary Video SV4
Supplementary Video SV5

References

1. Basson MA. Signaling in cell differentiation and morphogenesis. Cold Spring Harb Perspect Biol 2012;4(6): a008151.
2. Simin K, Bates EA, Horner MA, et al. Genetic analysis of punt, a type II Dpp receptor that functions throughout the *Drosophila melanogaster* life cycle. Genetics 1998; 148(2):801–813.
3. Letsou A, Arora K, Wrana JL, et al. Drosophila Dpp signaling is mediated by the punt gene product: A dual ligand-binding type II receptor of the TGF beta receptor family. Cell 1995;80(6):899–908.

4. Newfeld SJ, Mehra A, Singer MA, et al. Mothers against Dpp participates in a DDP/TGF-beta responsive serine-threonine kinase signal transduction cascade. Development 1997;124(16):3167–3176.
5. Chen Y, Riese MJ, Killinger MA, et al. A genetic screen for modifiers of Drosophila decapentaplegic signaling identifies mutations in punt, Mothers against Dpp and the BMP-7 homologue, 60A. Development 1998;125(9): 1759–1768.
6. Inoue H, Imamura T, Ishidou Y, et al. Interplay of signal mediators of decapentaplegic (Dpp): Molecular characterization of mothers against dpp, Medea, and daughters against dpp. Mol Biol Cell 1998;9(8):2145–2156.
7. Nohe A, Hassel S, Ehrlich M, et al. The mode of bone morphogenetic protein (BMP) receptor oligomerization determines different BMP-2 signaling pathways. J Biol Chem 2002;277(7):5330–5338.
8. Bolos V, Grego-Bessa J, de la Pompa JL. Notch signaling in development and cancer. Endocr Rev 2007;28(3):339–363.
9. Wang RN, Green J, Wang Z, et al. Bone Morphogenetic Protein (BMP) signaling in development and human diseases. Genes Dis 2014;1(1):87–105.
10. Srivastava P, Kane A, Harrison C, et al. A meta-analysis of bioelectric data in cancer, embryogenesis, and regeneration. Bioelectricity 2021;3(1):42–67.
11. Durant F, Bischof J, Fields C, et al. The role of early bioelectric signals in the regeneration of planarian anterior/posterior polarity. Biophys J 2019;116(5):948–961.
12. George LF, Pradhan SJ, Mitchell D, et al. Ion channel contributions to wing development in *Drosophila melanogaster*. G3 (Bethesda) 2019;9(4):999–1008.
13. Adams DS, Uzel SG, Akagi J, et al. Bioelectric signalling via potassium channels: A mechanism for craniofacial dysmorphogenesis in KCNJ2-associated Andersen-Tawil Syndrome. J Physiol 2016;594(12):3245–3270.
14. Simons C, Rash LD, Crawford J, et al. Mutations in the voltage-gated potassium channel gene KCNH1 cause Temple-Baraitser syndrome and epilepsy. Nat Genet 2015;47(1):73–77.
15. Perathoner S, Daane JM, Henrion U, et al. Bioelectric signaling regulates size in zebrafish fins. PLoS Genet 2014;10(1):e1004080.
16. Belus MT, Rogers MA, Elzubeir A, et al. Kir2.1 is important for efficient BMP signaling in mammalian face development. Dev Biol 2018;444(Suppl. 1):S297–S307.
17. Durant F, Morokuma J, Fields C, et al. Long-term, stochastic editing of regenerative anatomy via targeting endogenous bioelectric gradients. Biophys J 2017;112(10): 2231–2243.
18. Iovine MK, Higgins EP, Hindes A, et al. Mutations in connexin43 (GJA1) perturb bone growth in zebrafish fins. Dev Biol 2005;278(1):208–219.
19. Li A, Cho JH, Reid B, et al. Calcium oscillations coordinate feather mesenchymal cell movement by SHH dependent modulation of gap junction networks. Nat Commun 2018;9(1):5377.
20. Dahal GR, Rawson J, Gassaway B, et al. An inwardly rectifying K+ channel is required for patterning. Development 2012;139(19):3653–3664.
21. Bates E. Ion channels in development and cancer. Annu Rev Cell Dev Biol 2015;31:231–247.
22. Splawski I, Timothy KW, Decher N, et al. Severe arrhythmia disorder caused by cardiac L-type calcium channel mutations. Proc Natl Acad Sci U S A 2005; 102(23):8089–8096; discussion 6–8.
23. Splawski I, Timothy KW, Sharpe LM, et al. Ca(V)1.2 calcium channel dysfunction causes a multisystem disorder including arrhythmia and autism. Cell 2004;119(1): 19–31.
24. Yoon G, Oberoi S, Tristani-Firouzi M, et al. Andersen-Tawil syndrome: Prospective cohort analysis and expansion of the phenotype. Am J Med Genet A 2006;140(4): 312–321.
25. Donaldson MR, Yoon G, Fu YH, et al. Andersen-Tawil syndrome: A model of clinical variability, pleiotropy, and genetic heterogeneity. Ann Med 2004;36(Suppl. 1):92–97.
26. Yoon G, Quitania L, Kramer JH, et al. Andersen-Tawil syndrome: Definition of a neurocognitive phenotype. Neurology 2006;66(11):1703–1710.
27. Barel O, Shalev SA, Ofir R, et al. Maternally inherited Birk Barel mental retardation dysmorphism syndrome caused by a mutation in the genomically imprinted potassium channel KCNK9. Am J Hum Genet 2008;83(2): 193–199.
28. Nilius B, Voets T. The puzzle of TRPV4 channelopathies. EMBO Rep 2013;14(2):152–163.
29. Stray-Pedersen A, Sorte HS, Samarakoon P, et al. Primary immunodeficiency diseases: Genomic approaches delineate heterogeneous Mendelian disorders. J Allergy Clin Immunol 2017;139(1):232–245.
30. Al-Sayed MD, Al-Zaidan H, Albakheet A, et al. Mutations in NALCN cause an autosomal-recessive syndrome with severe hypotonia, speech impairment, and cognitive delay. Am J Hum Genet 2013;93(4):721–726.
31. Chong JX, McMillin MJ, Shively KM, et al. De novo mutations in NALCN cause a syndrome characterized by congenital contractures of the limbs and face, hypotonia, and developmental delay. Am J Hum Genet 2015;96(3): 462–473.
32. Hoppman-Chaney N, Wain K, Seger PR, et al. Identification of single gene deletions at 15q13.3: Further evidence that CHRNA7 causes the 15q13.3 microdeletion syndrome phenotype. Clin Genet 2013;83(4):345–351.
33. Bichet D, Haass FA, Jan LY. Merging functional studies with structures of inward-rectifier K(+) channels. Nat Rev Neurosci 2003;4(12):957–967.
34. Hibino H, Inanobe A, Furutani K, et al. Inwardly rectifying potassium channels: Their structure, function, and physiological roles. Physiol Rev 2010;90(1):291–366.
35. Braun M, Ramracheya R, Bengtsson M, et al. Voltage-gated ion channels in human pancreatic beta-cells: Electrophysiological characterization and role in insulin secretion. Diabetes 2008;57(6):1618–1628.
36. Misler S, Barnett DW, Gillis KD, et al. Electrophysiology of stimulus-secretion coupling in human beta-cells. Diabetes 1992;41(10):1221–1228.
37. Misler S, Barnett DW, Pressel DM, et al. Stimulus-secretion coupling in beta-cells of transplantable human islets of Langerhans. Evidence for a critical role for Ca2+ entry. Diabetes 1992;41(6):662–670.
38. Riz M, Braun M, Wu X, et al. Inwardly rectifying Kir2.1 currents in human beta-cells control electrical activity: Characterisation and mathematical modelling. Biochem Biophys Res Commun 2015;459(2):284–287.
39. Rorsman P, Braun M. Regulation of insulin secretion in human pancreatic islets. Annu Rev Physiol 2013;75:155–179.

40. Dahal GR, Pradhan SJ, Bates EA. Inwardly rectifying potassium channels influence Drosophila wing morphogenesis by regulating Dpp release. Development 2017; 144(15):2771–2783.
41. Ohno Y, Otaki JM. Spontaneous long-range calcium waves in developing butterfly wings. BMC Dev Biol 2015;15:17.
42. Narciso C, Wu Q, Brodskiy P, et al. Patterning of wound-induced intercellular Ca(2+) flashes in a developing epithelium. Phys Biol 2015;12(5):056005.
43. Restrepo S, Basler K. Drosophila wing imaginal discs respond to mechanical injury via slow InsP3R-mediated intercellular calcium waves. Nat Commun 2016;7:12450.
44. Balaji R, Bielmeier C, Harz H, et al. Calcium spikes, waves and oscillations in a large, patterned epithelial tissue. Sci Rep 2017;7:42786.
45. Brodskiy PA, Wu Q, Soundarrajan DK, et al. Decoding calcium signaling dynamics during drosophila wing disc development. Biophys J 2019;116(4):725–740.
46. Huang H, Liu S, Kornberg TB. Glutamate signaling at cytoneme synapses. Science 2019;363(6430):948–955.
47. Webb SE, Miller AL. Ca2+ signaling and early embryonic patterning during the blastula and gastrula periods of zebrafish and Xenopus development. Biochim Biophys Acta 2006;1763(11):1192–1208.
48. Wallingford JB, Ewald AJ, Harland RM, et al. Calcium signaling during convergent extension in Xenopus. Curr Biol 2001;11(9):652–661.
49. Nguyen NT, Han W, Cao WM, et al. Store-operated calcium entry mediated by ORAI and STIM. Compr Physiol 2018;8(3):981–1002.
50. Nguyen NT, Ma G, Lin E, et al. CRAC channel-based optogenetics. Cell Calcium 2018;75:79–88.
51. Manjarres IM, Rodriguez-Garcia A, Alonso MT, et al. The sarco/endoplasmic reticulum Ca(2+) ATPase (SERCA) is the third element in capacitative calcium entry. Cell Calcium 2010;47(5):412–418.
52. Abou Tayoun AN, Li X, Chu B, et al. The Drosophila SK channel (dSK) contributes to photoreceptor performance by mediating sensitivity control at the first visual network. J Neurosci 2011;31(39):13897–13910.
53. Barro-Soria R, Aldehni F, Almaca J, et al. ER-localized bestrophin 1 activates Ca2+-dependent ion channels TMEM16A and SK4 possibly by acting as a counterion channel. Pflugers Arch 2010;459(3):485–497.
54. Chien LT, Hartzell HC. Drosophila bestrophin-1 chloride current is dually regulated by calcium and cell volume. J Gen Physiol 2007;130(5):513–524.
55. Hazegh KE, Reis T. A Buoyancy-based method of determining fat levels in Drosophila. J Vis Exp 2016(117): 54744.
56. Feng Y, Ueda A, Wu CF. A modified minimal hemolymph-like solution, HL3.1, for physiological recordings at the neuromuscular junctions of normal and mutant Drosophila larvae. J Neurogenet 2004;18(2):377–402.
57. George LF, Bates EA. Imaging Dpp release from a drosophila wing disc. J Vis Exp 2019;(152); doi: 10.3791/60528
58. Sotillos S, De Celis JF. Interactions between the Notch, EGFR, and decapentaplegic signaling pathways regulate vein differentiation during Drosophila pupal wing development. Dev Dyn 2005;232(3):738–752.
59. Blair SS. Wing vein patterning in Drosophila and the analysis of intercellular signaling. Annu Rev Cell Dev Biol 2007;23:293–319.
60. Bosch PS, Ziukaite R, Alexandre C, et al. Dpp controls growth and patterning in Drosophila wing precursors through distinct modes of action. Elife 2017;6:e22546.
61. Hevia CF, de Celis JF. Activation and function of TGFbeta signalling during Drosophila wing development and its interactions with the BMP pathway. Dev Biol 2013;377(1):138–153.
62. Zacharioudaki E, Magadi SS, Delidakis C. bHLH-O proteins are crucial for Drosophila neuroblast self-renewal and mediate Notch-induced overproliferation. Development 2012;139(7):1258–1269.
63. Zacharioudaki E, Bray SJ. Tools and methods for studying Notch signaling in *Drosophila melanogaster*. Methods 2014;68(1):173–182.
64. Eid JP, Arias AM, Robertson H, et al. The Drosophila STIM1 orthologue, dSTIM, has roles in cell fate specification and tissue patterning. BMC Dev Biol 2008;8:104.
65. Suisse A, Treisman JE. Reduced SERCA function preferentially affects Wnt signaling by retaining E-cadherin in the endoplasmic reticulum. Cell Rep 2019;26(2):322.e3–329.e3.
66. Chen Y, Chen YF, Chiu WT, et al. The STIM1-Orai1 pathway of store-operated Ca2+ entry controls the checkpoint in cell cycle G1/S transition. Sci Rep 2016;6:22142.
67. Huang YW CS, Harn HI, Huang HT, et al. Mechanosensitive store-operated calcium entry regulates the formation of cell polarity. J Cell Physiol 2015;230(9): 2086–2097.
68. Short AD, Bian J, Ghosh TK, et al. Intracellular Ca2+ pool content is linked to control of cell growth. Proc Natl Acad Sci U S A 1993;90(11):4986–4990.
69. Everetts NJ, Worley MI, Yasutomi R, et al. Single-cell transcriptomics of the Drosophila wing disc reveals instructive epithelium-to-myoblast interactions. Elife 2021;10:e61276.
70. Ralston ABS. Long Range Dpp Signaling is regulated to restrict BMP signaling to a crossein competent zone. Dev Biol 2005;280:187–200.
71. Kawano S, Shoji S, Ichinose S, et al. Characterization of Ca(2+) signaling pathways in human mesenchymal stem cells. Cell Calcium 2002;32(4):165–174.
72. Kono T, Nishikori T, Kataoka H, et al. Spontaneous oscillation and mechanically induced calcium waves in chondrocytes. Cell Biochem Funct 2006;24(2):103–111.
73. Godin LM, Suzuki S, Jacobs CR, et al. Mechanically induced intracellular calcium waves in osteoblasts demonstrate calcium fingerprints in bone cell mechanotransduction. Biomech Model Mechanobiol 2007;6(6): 391–398.
74. Tsutsumi M, Inoue K, Denda S, et al. Mechanical-stimulation-evoked calcium waves in proliferating and differentiated human keratinocytes. Cell Tissue Res 2009; 338(1):99–106.
75. Justet C, Chifflet S, Hernandez JA. Calcium oscillatory behavior and its possible role during wound healing in bovine corneal endothelial cells in culture. Biomed Res Int 2019;2019:8647121.
76. Uhrenholt TR, Domeier TL, Segal SS. Propagation of calcium waves along endothelium of hamster feed arteries. Am J Physiol Heart Circ Physiol 2007;292(3): H1634–H1640.
77. Yokota Y, Nakajima H, Wakayama Y, et al. Endothelial Ca 2+ oscillations reflect VEGFR signaling-regulated angiogenic capacity in vivo. Elife 2015;4:e08817.

78. Nathanson MH. Cellular and subcellular calcium signaling in gastrointestinal epithelium. Gastroenterology 1994; 106(5):1349–1364.
79. Evans JH, Sanderson MJ. Intracellular calcium oscillations regulate ciliary beat frequency of airway epithelial cells. Cell Calcium 1999;26(3–4):103–110.
80. Evans JH, Sanderson MJ. Intracellular calcium oscillations induced by ATP in airway epithelial cells. Am J Physiol 1999;277(1):L30–L41.
81. Nihei OK, Campos de Carvalho AC, Spray DC, et al. A novel form of cellular communication among thymic epithelial cells: Intercellular calcium wave propagation. Am J Physiol Cell Physiol 2003;285(5):C1304–C1313.
82. Stewart TA, Davis FM. An element for development: Calcium signaling in mammalian reproduction and development. Biochim Biophys Acta Mol Cell Res 2019; 1866(7):1230–1238.
83. Lee SH PY, Song M, Srikanth S, et al. Orai1 mediates osteogenic differentiation via BMP signaling pathway in bone marrow mesenchymal stem cells. Biochem Biophys Res Commun 2016;473(4):1309–1314.
84. Lacruz RS, Feske S. Diseases caused by mutations in ORAI1 and STIM1. Ann N Y Acad Sci 2015;1356: 45–79.
85. Morin G, Bruechle NO, Singh AR, et al. Gain-of-function mutation in STIM1 (P.R304W) is associated with stormorken syndrome. Hum Mutat 2014;35(10):1221–1232.
86. McCarl CA, Picard C, Khalil S, et al. ORAI1 deficiency and lack of store-operated Ca2+ entry cause immunodeficiency, myopathy, and ectodermal dysplasia. J Allergy Clin Immunol 2009;124(6):1311.e7–1318.e7.
87. Roti G, Carlton A, Ross KN, et al. Complementary genomic screens identify SERCA as a therapeutic target in NOTCH1 mutated cancer. Cancer Cell 2013;23(3): 390–405.
88. Le Bras S, Rondanino C, Kriegel-Taki G, et al. Genetic identification of intracellular trafficking regulators involved in Notch-dependent binary cell fate acquisition following asymmetric cell division. J Cell Sci 2012; 125(Pt 20):4886–4901.
89. Periz G, Fortini ME. Ca(2+)-ATPase function is required for intracellular trafficking of the Notch receptor in Drosophila. EMBO J 1999;18(21):5983–5993.
90. Banerjee S, Lee J, Venkatesh K, et al. Loss of flight and associated neuronal rhythmicity in inositol 1,4,5-trisphosphate receptor mutants of Drosophila. J Neurosci 2004;24(36):7869–7878.
91. Karagas NE, Venkatachalam K. Roles for the endoplasmic reticulum in regulation of neuronal calcium homeostasis. Cells 2019;8(10):1232.
92. Draznin B. Intracellular calcium, insulin secretion, and action. Am J Med 1988;85(5A):44–58.
93. Katz B, Miledi R. Ionic requirements of synaptic transmitter release. Nature 1967;215(5101):651.
94. Sudhof TC. Calcium control of neurotransmitter release. Cold Spring Harb Perspect Biol 2012;4(1):a011353.
95. Chow RH, von Ruden L, Neher E. Delay in vesicle fusion revealed by electrochemical monitoring of single secretory events in adrenal chromaffin cells. Nature 1992; 356(6364):60–63.
96. Voets T. Dissection of three Ca2+-dependent steps leading to secretion in chromaffin cells from mouse adrenal slices. Neuron 2000;28(2):537–545.
97. Alvarez J. Calcium dynamics in the secretory granules of neuroendocrine cells. Cell Calcium 2012;51(3–4):331–337.
98. Klec C, Ziomek G, Pichler M, et al. Calcium signaling in ss-cell physiology and pathology: A revisit. Int J Mol Sci 2019;20(24):6110.
99. Xiong QY, Yu C, Zhang Y, et al. Key proteins involved in insulin vesicle exocytosis and secretion. Biomed Rep 2017;6(2):134–139.
100. Wu B, Guo W. The exocyst at a glance. J Cell Sci 2015; 128(16):2957–2964.
101. Michel M, Raabe I, Kupinski AP, et al. Local BMP receptor activation at adherens junctions in the Drosophila germline stem cell niche. Nat Commun 2011;2:415.
102. Mao Y, Tu R, Huang Y, et al. The exocyst functions in niche cells to promote germline stem cell differentiation by directly controlling EGFR membrane trafficking. Development 2019;146(13):dev174615.
103. Sorre B, Warmflash A, Brivanlou AH, et al. Encoding of temporal signals by the TGF-beta pathway and implications for embryonic patterning. Dev Cell 2014;30(3):334–342.
104. Sagner A, Briscoe J. Morphogen interpretation: Concentration, time, competence, and signaling dynamics. Wiley Interdiscip Rev Dev Biol 2017;6(4):e271.
105. Sehgal P, Szalai P, Olesen C, et al. Inhibition of the sarco/endoplasmic reticulum (ER) Ca(2+)-ATPase by thapsigargin analogs induces cell death via ER Ca(2+) depletion and the unfolded protein response. J Biol Chem 2017;292(48):19656–19673.
106. Wang F, Liu DZ, Xu H, et al. Thapsigargin induces apoptosis by impairing cytoskeleton dynamics in human lung adenocarcinoma cells. Sci World J 2014;2014: 619050.
107. Davidson GA, Varhol RJ. Kinetics of thapsigargin-Ca(2+)-ATPase (sarcoplasmic reticulum) interaction reveals a two-step binding mechanism and picomolar inhibition. J Biol Chem 1995;270(20):11731–11734.

Address correspondence to:
Emily Anne Bates, PhD
Department of Pediatrics
University of Colorado Anschutz Medical Campus
12800 E. 19th Avenue, MS 8313
Aurora, CO 80045
USA

Email: emily.bates@cuanschutz.edu